AIAA SciTech Forum
12-16 January 2026, Orlando, FL
AIAA SCITECH 2026 Forum

10.2514/6.2026-2606

A CFD study of the combustion process in a miniature shock tube at different oxyhydrogen fill pressures

Janardhanraj Subburaj *, Touqeer Anwar Kashif †, Michael Vogl‡, Sanskar Maddi§, Zainab Alyousef¶ and Aamir Farooq‖

Mechanical Engineering, Physical Sciences and Engineering (PSE) Division, King Abdullah University of Science and Technology (KAUST), Thuwal, 23955-6900, Saudi Arabia

Miniature shock and detonation tubes are increasingly used for blast-wave generation, materials testing, and ignition of advanced propulsion systems. This study presents a detailed computational investigation of combustion and wave propagation in a 6 mm-diameter, 165 mm-long shock tube charged with hydrogen–oxygen mixtures at varying equivalence ratios and nitrogen dilution levels. Using a three-dimensional CFD framework with detailed chemical kinetics and adaptive mesh refinement, key flame dynamics across regimes from slow deflagration to detonations are captured. The simulations reproduce experimental observations of impulse generation and pressure evolution, and demonstrate sensitivity of the combustion mode to mixture composition and fill pressure. These findings lay the groundwork for optimizing miniature shock tube design for a broad range of scientific and engineering applications.

I. Background & Aim

Miniature shock and detonation tubes are increasingly recognized as versatile platforms for generating precisely controlled, high-intensity shock waves, with a broad range of applications across multiple disciplines [1, 2]. Their compact geometry and repeatable high-pressure generation over short durations enable controlled material testing, dynamic deformation studies, and synthesis of advanced materials for harsh environments. [3–5]. Beyond materials science, miniature shock tubes have demonstrated utility in biological applications, where the pressure profiles provide excellent reproducibility and precise control for procedures such as bacterial transformation and needle-free vaccine or drug delivery. [6, 7]. The scalability and operational simplicity of miniature shock tubes have also inspired their integration into micro-scale propulsion systems, including micro-pulsed detonation engines (μPDEs) and micro-propulsion thrusters [8, 9]. Han et al. [8] developed a μPDE of 4.22 mm inner diameter capable of sustained operation at 5 Hz using an ethylene–oxygen mixture while Lee and co-workers [9] optimized a 3.86 mm–diameter, 155 mm–long μPDE using high-speed schlieren imaging and wall-pressure measurements to refine operating parameters for hydrogen–oxygen mixtures.

With recent developments in aerospace propulsion, miniature shock and detonation tubes are gaining significant interest as igniters and pre-detonators for advanced combustion systems. In particular, rotating detonation engines (RDEs) require robust, repeatable ignition mechanisms to reliably initiate self-sustained detonation waves in the main combustor, for which compact hydrogen–oxygen pre-detonator tubes are attractive candidates [10, 11]. In such configurations, a small pre-detonator can generate a detonation that is injected tangentially or axially into an annular or linear combustor to seed one or more rotating detonation fronts, as demonstrated in recent numerical and experimental studies [11, 12]. Hydrogen–oxygen mixtures offer rapid deflagration-to-detonation transition (DDT), high energy density, and good compatibility with aerospace systems; importantly, they can be operated over a relatively wide equivalence ratio range while maintaining reliable detonation propensity [13]. However, it should be noted that the utility of miniature shock tubes extends beyond serving as igniters for propulsion. These devices also act as general platforms to study and harness fast combustion and shockwave phenomena on small scales, enabling insights into flame acceleration, pressure wave generation, and impulse delivery that are relevant to diverse end-use applications.

Several recent studies have begun to characterize the performance of miniature shock tubes and identify key dynamics driving their behavior. Janardhanraj et al. [14, 15] documented blast-wave profiles from a miniature tube utilizing

*Research Scientist, CERP, janardhanraj.subburaj@kaust.edu.sa, AIAA Senior Member.
†Postdoctoral Fellow, CERP, touqeer.kashif@kaust.edu.sa.
‡Visiting Student, CERP,michael.vogl@kaust.edu.sa..
§PhD student, CERP,sanskar.maddi@kaust.edu.sa.
¶Visiting Student, CERP,zainab.alyousef1@@kaust.edu.sa.
‖Professor, CERP, aamir.farooq@kaust.edu.sa.

in situ electrolysis to generate oxyhydrogen mixtures at fill pressures of 14–18 psi. In a related study, Janardhanraj et al. [16] reported on a 165 mm miniature shock tube, characterizing both impulse generation and combustion dynamics. On the modeling front, analytical and numerical investigations over the past decades have established fundamental insights into pulse detonation tube performance [17–19]. Wintenberger et al. developed an analytical model for the impulse of a single-cycle detonation tube, providing a baseline for evaluating the energy release and thrust potential of pulsed detonation devices [17]. Building on such foundations, high-fidelity CFD frameworks now enable multidimensional simulations of reactive shock propagation in geometries representative of miniature tubes. Commercial solvers like CONVERGE CFD have been successfully employed to capture shock formation and propagation in shock-tube configurations [20–22]. Likewise, Pal et al. applied large-eddy simulations to resolve the complex flow and combustion dynamics in a hydrogen–air rotating detonation engine, demonstrating the effectiveness of detailed chemistry and adaptive mesh refinement in capturing detonation phenomena [23]. However, despite these advances, there remains a shortage of validated numerical studies focused specifically on miniature hydrogen–oxygen shock and detonation tubes at millimeter-scale diameters. In this regime, strong confinement, significant wall heat losses, and incomplete coupling between the leading shock and the reaction zone can strongly influence the wave propagation behavior, often resulting in slow deflagration waves (flame fronts) instead of a self-sustained Chapman–Jouguet detonation even for ostensibly detonable mixtures. This gap highlights the need for a dedicated computational framework that can capture the unique thermochemical and gas-dynamic interplay in miniature tubes, and thus help guide their design and operation.

The objective of the present work is to develop and validate a three-dimensional CFD framework for modeling combustion and wave propagation in a miniature shock tube filled with hydrogen–oxygen mixtures at different dilution levels and initial fill pressures. A 6 mm diameter, 165 mm long tube is simulated using CONVERGE CFD with Reynolds-averaged Navier–Stokes turbulence modeling, adaptive mesh refinement, and detailed chemistry to capture the coupled thermochemical and gas-dynamic processes governing wave evolution. These conditions are chosen to systematically probe the device's behavior from highly reactive cases to marginal detonation cases, and were motivated by previous experimental measurements on similar miniature shock tubes [14, 16]. Overall, the CFD framework demonstrated here captures the key thermochemical and flow features governing miniature shock-tube operation. By quantifying the sensitivity of the shock tube's performance to the initial fill pressure and mixture dilution, the present study provides a robust computational foundation for predictive design and optimization of miniature shock/detonation tubes across different operating regimes and applications. In addition to guiding the design of miniature pre-detonator igniters for propulsion systems, the insights from this work can be leveraged to enhance miniature shock tube effectiveness in materials processing, biomedical energy delivery, and other emerging applications where controlled blast-wave generation is desired.

II. Methodology

The numerical simulations in this study were performed using the commercial CFD solver CONVERGE, and were designed to replicate a previously studied miniature shock tube configuration [14] with the goal of enabling future experimental validation. The geometry of the computational domain is shown in Fig 1 and consists of a three-dimensional, axisymmetric cylindrical tube of 6 mm internal diameter and 165 mm total length. This configuration closely mirrors the physical prototype reported in prior experimental work. To initiate the combustion process, a volumetric ignition zone was defined 15 mm from the closed end of the tube to mimic the placement of a Rimfire Z3 miniature spark plug used in prior studies. The ignition was modeled by introducing a spherical source of 1 mm diameter with an energy deposition of 2 mJ, in line with ignition system used to power the spark plug. The duration of the ignition source was set to 10 microseconds and the maximum temperature was limited to 5000 K. The computational domain boundaries were treated with isothermal no-slip wall conditions, with wall temperature fixed at 294.6 K to emulate ambient laboratory conditions. The governing equations were the Reynolds-Averaged Navier–Stokes (RANS) equations with the k–ω Shear Stress Transport (SST) turbulence model. Wall heat transfer was modeled using the O'Rourke and Amsden correlation, along with standard wall functions for both velocity and thermal boundary layers.

The chemical kinetics of combustion were resolved using the SAGE detailed chemistry solver, incorporating the GRIMech 3.0 mechanism, which includes 53 species and 325 reactions relevant for hydrogen–oxygen–nitrogen combustion. Spatial discretization used a second-order MUSCL scheme, while temporal discretization was governed by an adaptive timestep controller with a maximum Courant–Friedrichs–Lewy (CFL) number of 0.9 to ensure numerical stability. A base mesh size of 250 μm was applied throughout the domain, with adaptive mesh refinement (AMR) triggered in regions of steep pressure and temperature gradients, allowing for local cell sizes as fine as 31.25 μm. This fine resolution enabled accurate capture of ignition kernel evolution, flame front propagation, and the transition from

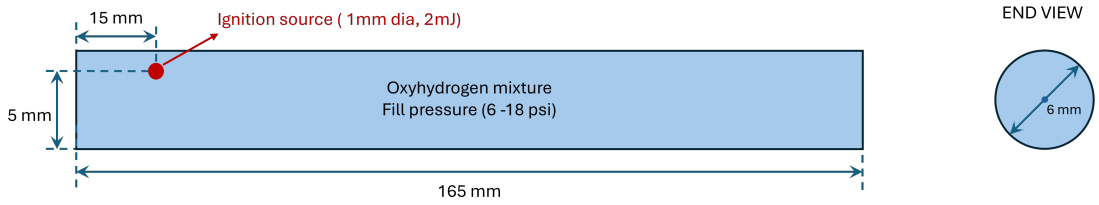

Fig. 1 Schematic of the three-dimensional computational domain used in the CFD simulations. The tube geometry consists of a 6 mm internal diameter and 165 mm total length, with a spherical ignition kernel placed 15 mm from the closed end to replicate the location of a Rimfire Z3 miniature spark plug.

deflagration to detonation where applicable. Initial fill pressures and gas compositions were selected to systematically span a range of reactivities and detonation regimes, based on conditions studied in previous experimental efforts. These are summarized in Table 1, which details the hydrogen, oxygen, and nitrogen mole fractions used in each simulation case, the corresponding equivalence ratio, and whether a detonation was observed.

Table 1 Simulation cases with varying fuel–oxidizer–diluent compositions (expressed in mole fractions), corresponding equivalence ratios (ϕ), and observed detonation occurrence. These configurations were chosen to span a range of mixture reactivities and highlight transitions between deflagration and detonation.

Case #	H_2 (%)	O_2 (%)	N_2 (%)	Equivalence ratio, ϕ	Detonation Occurrence
1	29.57	14.78	55.63		×
2	36.31	18.15	45.53	1	✓
3	47.01	23.50	29.47		✓
4	66.66	33.33	0		✓
5	38.65	12.88	48.46		×
6	46.09	15.365	38.53	1.5	✓
7	57.09	19.03	23.86		✓
8	75	25	0		✓

III. Results and Discussions

Figure 2 presents the pressure histories at the tube's end for all simulated mixtures (see Table 1 for compositions). Time zero corresponds to the ignition event via the ignition source described int he previous section. For the stoichiometric mixtures (ϕ = 1, Fig. 2a), the case with the highest N_2 dilution (55.63% N_2, black curve) exhibits a gradual pressure rise to about 2 MPa over several hundred microseconds, followed by mild oscillations reaching 4 MPa. The initial flame front does not show a sharp jump (typical of a detonation) in this highly diluted case; instead, the flame propagates as a deflagration, and the modest pressure increase is due to the confined flame compressing the unburned gas. This distributed, multi-peaked pressure profile contrasts sharply with the single, intense pulse expected from a detonation, indicating a significantly lower impulse in the most diluted mixture. The flame development for the above non-detonating case is illustrated in Figure 3, which shows temperature contours on a central slice of the tube. At t = 30 μs, the ignition source (0.5 mm diameter, 2 mJ) initiates combustion. The flame then expands both radially and axially; by t = 700 μs, it has extended roughly halfway down the 165 mm tube, with burned-gas temperatures around 2500 K (near the adiabatic flame temperature). Under heavy dilution, a substantial portion of the combustion energy is absorbed by heating the inert N_2, so the flame's propagation is relatively slow and the burned gas temperature is lower than in less-diluted cases. The end-wall pressure rises correspondingly slowly during this period (black trace in Fig. 2a), increasing gradually until the flame front nears the tube's end. Subsequently, the flame's forward progress diminishes – it requires roughly an additional 1 ms to cover the final 25 mm of the tube length. Throughout this deflagration, no shock wave is produced; the pressure record remains a low-amplitude, extended pulse rather than a sharp detonation spike.

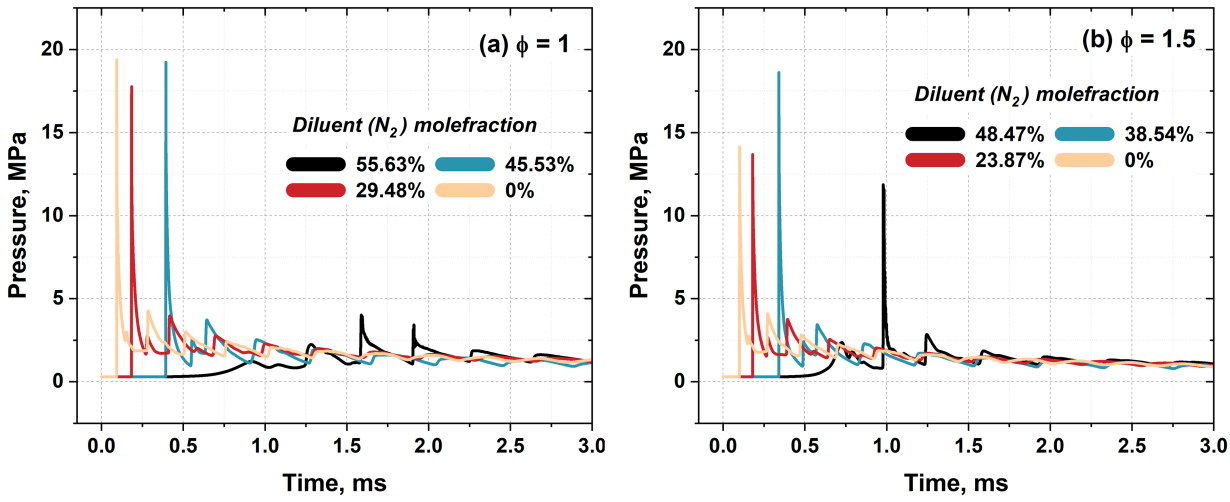

Fig. 2 Pressure histories at the end of the miniature tube for all simulated cases: (a) Cases 1–4 at equivalence ratio ϕ = 1; (b) Cases 5–8 at ϕ = 1.5. Highly diluted mixtures exhibit gradual pressure rise and weak combustion-induced compression, while cases with lower N_2 dilution or richer fuel content show sharp pressure spikes indicative of detonation. The timing and magnitude of the pressure rise reflect the mixture reactivity and combustion mode.

In contrast to the ϕ = 1 case above, a richer hydrogen–oxygen mixture (ϕ = 1.5) is more prone to detonation under similar conditions. For example, at ϕ = 1.5 with a high diluent level (Case 5, 48.5% N_2), the pressure trace (Fig. 2b, black curve) also begins with a slow deflagration-like rise. However, after the initial pressure peak, a sudden secondary spike occurs – the pressure surges to 10 MPa. This late-emerging high-pressure pulse indicates that a detonation eventually develops in the ϕ = 1.5, highly diluted mixture (whereas the ϕ = 1 counterpart never detonates). The likely scenario is that once the flame reached the tube's end in Case 5, pockets of unburned hydrogen–oxygen were abruptly consumed in a detonation, sending a shock back through the tube and producing the sharp pressure jump. This comparison suggests that the richer mixture can achieve detonation at a higher diluent concentration than the stoichiometric mixture – ϕ = 1.5 manages to detonate even with nearly 50% N_2, whereas ϕ = 1 fails to detonate at 55% N_2. Reducing the nitrogen dilution further leads to prompt detonation in both ϕ = 1 and ϕ = 1.5 cases. At lower N_2 levels (higher fuel/oxygen content), the pressure histories show an abrupt rise characteristic of a detonation shock arriving at the tube end. In these runs, a strong single pressure pulse is recorded, with peak pressures on the order of 10–15 MPa. Notably, the highest peak (15 MPa) occurs for the undiluted hydrogen-oxygen mixture and is consistent with the expected Chapman–Jouguet (CJ) detonation strength. The timing of detonation also shifts with composition: as the diluent fraction decreases, the detonation (shock) appears earlier in time (the arrival is a few tens of microseconds sooner for each step reduction in N_2). The peak pressure magnitudes do not follow a strict monotonic trend with dilution, likely due to complex wave–flame interactions and the dynamics of shock reflection. Overall, the results show that leaner (highly diluted) mixtures yield longer combustion durations and lower pressure peaks, whereas mixtures with less dilution (and/or richer ϕ) transition to detonation quickly, producing strong, impulsive pressure spikes.

Figure 4 provides a closer look at the flame's transition to detonation in a representative low-dilution case (ϕ = 1, 45.5% N_2). Early in this case, the flame evolution resembles that of the highly diluted scenario: at t = 30 μs a flame kernel is present near the ignition point, and by t = 120 μs the flame has propagated about 125 mm (approximately 75% of the tube length) as a subsonic deflagration. A key difference, however, is the flame temperature – with less inert gas to heat, the reaction zone here achieves a higher temperature than in the more diluted case (compare Figs. 4 and 3). This elevated energy release eventually drives a deflagration-to-detonation transition (DDT). At approximately t = 140 μs, a detonation wave forms at the flame front (Fig. 4, 140 μs panel) and the combustion mode shifts from deflagration to detonation. Once the flame transitions, the newly formed detonation front sweeps through the remaining unburned mixture at high velocity, essentially catching up to the tube's end in a matter of a few tens of microseconds. By t = 200 μs, the detonation wave has traversed the last portion of the tube and reaches the end. The burned gas behind this detonation front is at much higher pressure and temperature than in the earlier deflagration phase. Upon reaching

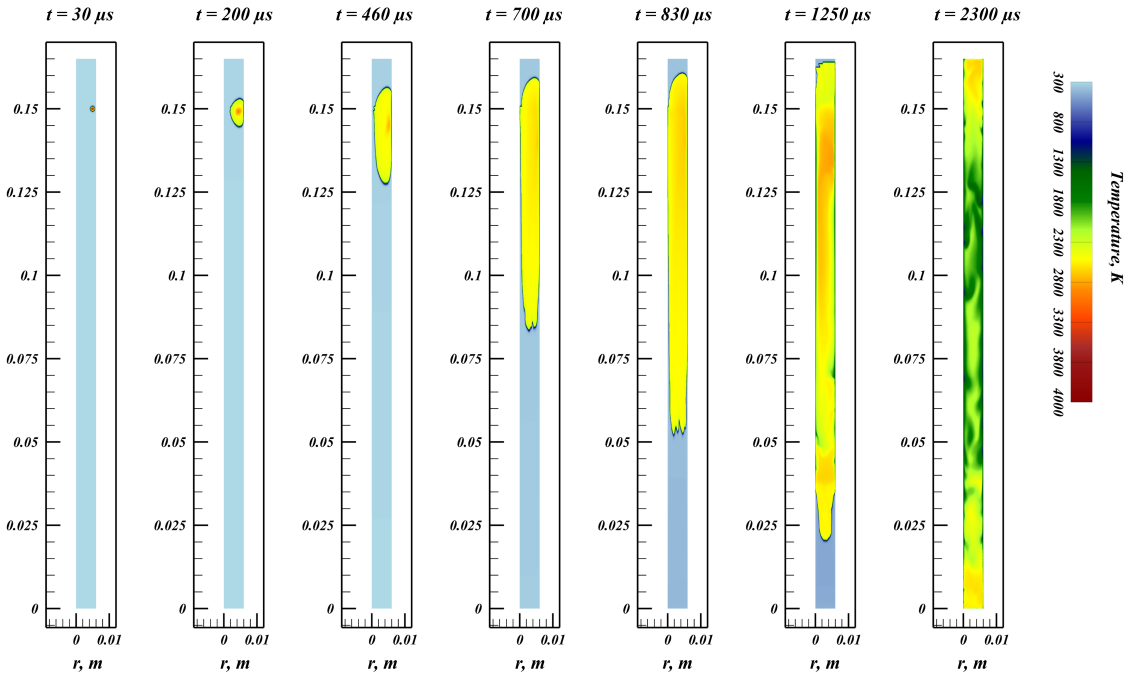

Fig. 3 Temperature contours for a deflagrating flame (Case 1: ϕ = 1, $H_2/O_2/N_2$ = 29.57%/14.78%/55.63%). The flame grows slowly along the axial direction, with no evidence of detonation. The extended combustion duration and modest post-flame temperatures (2500 K) are characteristic of heavily diluted mixtures and support the pressure observations in Figure 2a.

the tube end, the detonation wave undergoes a reflection/expansion (depending on end conditions), which causes a secondary compression in the tube and further increases the gas temperature immediately behind the reflected wave. This sequence in Fig. 4 illustrates how a flame in a miniature tube can transition from a slow burn to a detonation given sufficient energy release rate and confinement. The ϕ = 1.5 cases follow a qualitatively similar sequence – all ϕ = 1.5 mixtures with moderate or low dilution undergo DDT as well – but the richer fuel mixtures tend to detonate slightly sooner (in time and distance) than their ϕ = 1 counterparts due to higher reactivity. In summary, decreasing diluent fraction and increasing equivalence ratio both promote earlier DDT, which in turn yields a more abrupt and high-magnitude pressure pulse (greater impulse) compared to the gentler pressure buildup of a deflagration.

To further characterize the flame propagation and detonation onset, flame-front velocities were measured along the tube for selected cases (Fig. 5). These velocities were obtained by placing virtual probes along the tube axis and tracking the time of arrival of the OH radical (a marker of the reaction zone). The resulting flame speed profiles clearly show the acceleration of the flame as it travels down the tube. For ϕ = 1 (black symbols in Fig. 5), the flame starts at a low speed (reflecting a subsonic deflagration) near the ignition end and gradually accelerates as it propagates downstream. Beyond the midpoint of the tube, a steep rise in velocity is observed, corresponding to the onset of detonation. By the time the flame reaches the tube exit, it is traveling at 2200 m/s, essentially the CJ detonation speed for the H_2/O_2 mixture. A similar trend is seen for the ϕ = 1.5 cases (red symbols), but with two notable differences: (1) the flame achieves higher intermediate speeds sooner, and (2) the deflagration-to-detonation transition occurs earlier along the tube (i.e. at a shorter distance from ignition) compared to the ϕ = 1 case. Ultimately, the ϕ = 1.5 flames also approach a terminal velocity on the order of 2000–2500 m/s once detonation is established, comparable to the ϕ = 1 case. This reflects the fact that after detonation onset, the flame front effectively becomes a self-sustained detonation wave, whose speed is dictated by the mixture's detonation properties rather than the initial flame speed. Indeed, once the flame transitions to a detonation, all common measures of flame speed converge to the detonation wave speed. The Figure 5 data thus reinforce the earlier observations: in mixtures that detonate, the flame accelerates rapidly to supersonic speeds, whereas in highly diluted non-detonating mixtures the flame would remain in the low-speed deflagration regime.

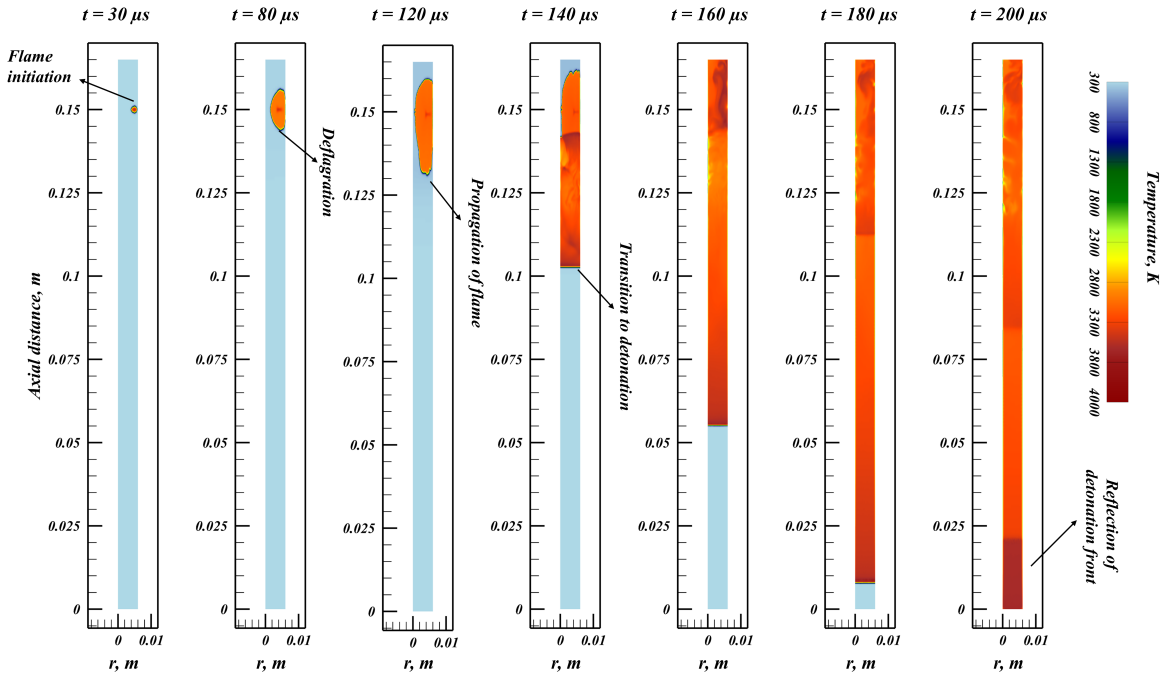

Fig. 4 Temperature contours for a detonating flame (Case 2: ϕ = 1, $H_2/O_2/N_2$ = 36.31%/18.15%/45.53%). Initially, the flame propagates as a deflagration, but transitions to detonation around 140 μs after ignition. The detonation front rapidly consumes the unburned mixture, resulting in strong temperature rise and secondary compression after reflection from the end wall. This case demonstrates deflagration-to-detonation transition (DDT) in a moderately diluted mixture.

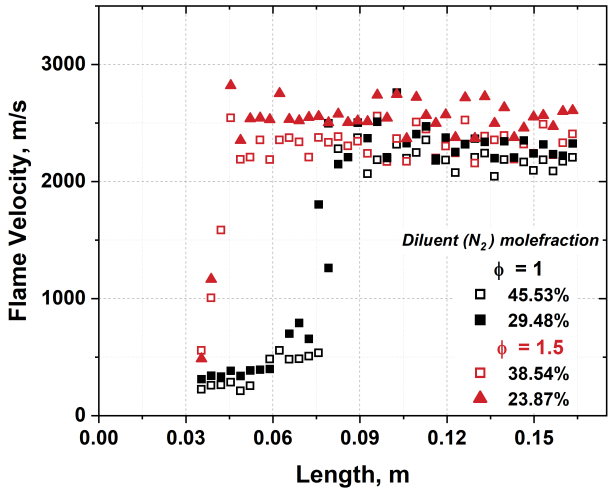

Fig. 5 Flame velocity measured along the miniature tube as a function of axial distance for selected $H_2/O_2/N_2$ mixtures at $\phi = 1$ (black symbols) and $\phi = 1.5$ (red symbols). Open and filled markers denote different N_2 diluent mole fractions as indicated in the legend.

IV. Summary and Future Work

This study develops and applies a high-fidelity CFD framework to analyze the combustion and wave propagation characteristics in a miniature shock tube filled with hydrogen–oxygen mixtures of varying compositions. The pressure

traces, flame speeds, and detonation onset at these compositions highlight the role of mixture dilution and equivalence ratio in determining the combustion regime. In cases with high nitrogen dilution, deflagration dominates, leading to a slow pressure build-up and low impulse, while richer or less diluted mixtures undergo deflagration-to-detonation transition (DDT), resulting in sharp pressure spikes and higher impulse. The results affirm the predictive capability of the CFD model in capturing flame development and detonation physics under strongly confined conditions, providing insights that are crucial for optimizing the operational characteristics of miniature shock tubes across diverse applications.

Future work involves completing a comprehensive experimental campaign to validate the simulation results. Specific objectives include:

- Validation of pressure profiles, flame speeds, and impulse measurements through experiments under varying fill pressures and mixture compositions.
- High-speed imaging and schlieren visualization to confirm wave propagation and detonation transition observed in simulations.
- Model refinement by incorporating more accurate boundary conditions and improved ignition models based on real spark plug behavior.
- Parameter mapping and scaling laws development for performance prediction across a broader operational range.

The present study will enhance the utility of the computational framework and guide the design of miniature shock tubes tailored for specific end-use scenarios, including pre-detonators for propulsion, impulse generators for material testing, and controlled delivery systems for biomedical applications

Acknowledgments

This work was funded by the Office of Sponsored Research at King Abdullah University of Science and Technology (KAUST).

References

[1] Janardhanraj, S., and Jagadeesh, G., "Development of a novel miniature detonation-driven shock tube assembly that uses in situ generated oxyhydrogen mixture," *Review of Scientific Instruments*, Vol. 87, No. 8, 2016. https://doi.org/10.1063/1.4960961, 085114.

[2] Janardhanraj, S., Abhishek, K., and Jagadeesh, G., "Insights into the shockwave attenuation in miniature shock tubes," *Journal of Fluid Mechanics*, Vol. 910, 2021, p. A3. https://doi.org/10.1017/jfm.2020.914.

[3] Bisht, A., Kumar, L., Subburaj, J., Jagadeesh, G., and Suwas, S., "Effect of stacking fault energy on the evolution of microstructure and texture during blast assisted deformation of FCC materials," *Journal of Materials Processing Technology*, Vol. 271, 2019, pp. 568–583. https://doi.org/https://doi.org/10.1016/j.jmatprotec.2019.04.029.

[4] Maity, T. N., Gopinath, N. K., Janardhanraj, S., Biswas, K., and Basu, B., "Computational and Microstructural Stability Analysis of Shock Wave Interaction with NbB2-B4C-Based Nanostructured Ceramics," *ACS Applied Materials & Interfaces*, Vol. 11, No. 50, 2019, pp. 47491–47500. https://doi.org/10.1021/acsami.9b13995.

[5] Bisht, A., Subburaj, J., Jagadeesh, G., and Suwas, S., "Deformation Behavior of Commercially Pure Titanium Subjected to Blast Assisted Deformation: New Insights on 11-21 Extension Twinning," *MATERIALS TRANSACTIONS*, Vol. 66, No. 5, 2025, pp. 521–531. https://doi.org/10.2320/matertrans.MT-MC2024010.

[6] Subburaj, J., Datey, A., Gopalan, J., and Chakravortty, D., "Insights into the mechanism of a novel shockwave-assisted needle-free drug delivery device driven by in situ-generated oxyhydrogen mixture which provides efficient protection against mycobacterial infections," *Journal of Biological Engineering*, Vol. 11, No. 1, 2017, p. 48. https://doi.org/10.1186/s13036-017-0088-x.

[7] Datey, A., Subburaj, J., Gopalan, J., and Chakravortty, D., "Mechanism of transformation in Mycobacteria using a novel shockwave assisted technique driven by in-situ generated oxyhydrogen," *Scientific Reports*, Vol. 7, No. 1, 2017, p. 8645. https://doi.org/10.1038/s41598-017-08542-5.

[8] Han, H.-S., Kim, J.-M., Oh, S., and Choi, J.-Y., "An Experimental Study on Characteristics of Small-scale PDE under Low-frequency Operating Conditions," *Journal of the Korean Society of Propulsion Engineers*, Vol. 22, No. 3, 2018. https://doi.org/10.6108/KSPE.2018.22.3.081.

[9] Lee, K.-H., Lee, J.-H., Kim, M.-S., Lee, E.-S., Han, H.-S., and Choi, J.-Y., "An Experimental Study on the Ignition of Scramjet Combustor using μPDE," *14th Asia-Pacific Conference on Combustion, Taiwan*, 2023.

[10] Lee, J.-H., Lee, E.-S., Han, H.-S., Kim, M.-S., and Choi, J.-Y., "A Study on a Vitiated Air Heater for a Direct-Connect Scramjet Combustor and Preliminary Test on the Scramjet Combustor Ignition," *Aerospace*, Vol. 10, No. 5, 2023. https://doi.org/10.3390/aerospace10050415.

[11] Pathangae, A. P., and Varadachari, R., "Numerical simulations of a hydrogen-air pre-detonator for detonation engines," *Proceedings of the Institution of Mechanical Engineers, Part G: Journal of Aerospace Engineering*, Vol. 238, No. 7, 2024, pp. 677–686. https://doi.org/10.1177/09544100241233324.

[12] Xue, S., Zhang, X., Yang, J., Liu, D., Ma, H., and Zhou, C., "Experimental study on the rotating detonation engine based on a gas mixture," *Frontiers in Energy Research*, Vol. Volume 11 - 2023, 2023. https://doi.org/10.3389/fenrg.2023.1136156.

[13] Armbruster, W., Bard, E., Boulal, S., Börner, M., General, S., Bee, A., and Hardi, J. S., "Design and testing of a hydrogen–oxygen pre-detonator for rotating detonation engines," 2025, pp. 969–979. https://doi.org/10.1007/s12567-025-00605-y.

[14] Subburaj, J., Sausa, A. R. P., and Farooq, A., "A Combustion-Driven Miniature Shock Tube With In-Situ Oxyhydrogen Generation: Energy and Impulse Analysis," *AIAA SCITECH 2025 Forum*, 2025, p. 2141. https://doi.org/10.2514/6.2025-2141.

[15] Janardhanraj, S., and Jagadeesh, G., "Energy Analysis of a Small-Scale Combustion Driven Blast Tube," *29th International Symposium on Shock Waves 1*, edited by R. Bonazza and D. Ranjan, Springer International Publishing, Cham, 2015, pp. 119–125. https://doi.org/10.1007/978-3-319-16835-7_17.

[16] Subburaj, J., Ngo, T., Sausa, A. R. P., and Farooq, A., "Combustion Characteristics and Impulse Generation in a Miniature Detonation Tube Driven by in-situ Generated Hydrogen-Oxygen Mixture," *AIAA SCITECH 2024 Forum*, 2024, p. 0586. https://doi.org/10.2514/6.2024-0586.

[17] Wintenberger, E., Austin, J., Cooper, M., Jackson, S., and Shepherd, J., "Analytical model for the impulse of single-cycle pulse detonation tube," *Journal of propulsion and power*, Vol. 19, No. 1, 2003, pp. 22–38. https://doi.org/10.2514/2.6099.

[18] Nicholls, J. A., Wilkinson, H. R., and Morrison, R. B., "Intermittent Detonation as a Thrust-Producing Mechanism," *Journal of Jet Propulsion*, Vol. 27, No. 5, 1957, pp. 534–541. https://doi.org/10.2514/8.12851.

[19] Zitoun, R., and Desbordes, D., "Propulsive Performances of Pulsed Detonations," *Combustion Science and Technology*, Vol. 144, No. 1-6, 1999, pp. 93–114. https://doi.org/10.1080/00102209908924199.

[20] Kashif, T. A., Subburaj, J., Ali Khan, M. Z., and Farooq, A., "Double-Diaphragm Induced Shock Velocity Variation and Its Effects on Shocked Gas," *AIAA Journal*, Vol. 63, No. 12, 2025, pp. 5059–5072. https://doi.org/10.2514/1.J065401.

[21] Kashif, T. A., Subburaj, J., Khan, M. Z. A., and Farooq, A., "Experimental and Numerical Study of Shock Dynamics in Double Diaphragm Shock Tubes," *AIAA SCITECH 2025 Forum*, 2025, p. 2145. https://doi.org/10.2514/6.2025-2145.

[22] Kashif, T. A., Subburaj, J., and Farooq, A., "On the flow characteristics in the shock formation region due to the diaphragm opening process in a shock tube," *Physics of Fluids*, Vol. 37, No. 6, 2025, p. 066117. https://doi.org/10.1063/5.0267878.

[23] Pal, P., Braun, J., Wang, Y., Athmanathan, V., Paniagua, G., and Meyer, T. R., "Large-Eddy Simulation Study of Flow and Combustion Dynamics in a Full-Scale Hydrogen–Air Rotating Detonation Combustor-Stator Integrated System," *Journal of Engineering for Gas Turbines and Power*, Vol. 147, No. 3, 2024, p. 031002. https://doi.org/10.1115/1.4066365.